

Identification of the heterogeneous conductivity in an inverse heat conduction problem

Angel Ciarbonetti^{*1}, Sergio Idelsohn^{†2}, and Ruben D. Spies^{‡1,3}

¹Instituto de Matemática Aplicada del Litoral, IMAL, CONICET-UNL, Centro Científico Tecnológico CONICET-Santa Fe, Argentina

²CIMNE International Centre for Numerical Methods in Engineering, Barcelona, Spain

³Departamento de Matemática, Facultad de Ingeniería Química, Universidad Nacional del Litoral, Santa Fe, Argentina

August 25, 2022

Abstract

This work deals with the problem of determining a non-homogeneous heat conductivity profile in a steady-state heat conduction boundary-value problem with mixed Dirichlet-Neumann boundary conditions over a bounded domain in \mathbb{R}^n , from the knowledge of the state over the whole domain. We develop a method based on a variational approach leading to an optimality equation which is then projected into a finite dimensional space. Discretization yields a linear although severely ill-posed equation which is then regularized via appropriate ad-hoc penalizers resulting in a generalized Tikhonov-Phillips functional. No smoothness assumptions are imposed on the conductivity. Numerical examples for the case in which the conductivity can take only two prescribed values (a two-materials case) show that the approach is able to produce very good reconstructions of the exact solution.

Keyword: *Heat-conduction, Elliptic Boundary-value Problem, Inverse Problems, Regularization, Tikhonov-Phillips, Thermal Materials Design*

1 Introduction

The study, analysis and numerical solution of *Inverse Heat Transfer Problems* (IHTP), has a significant role in a large number of engineering applications. Aerospace, mechanical, chemical and nuclear engineering, materials design, are just few of the many areas in which developing appropriate and efficient tools for solving IHTP is of special interest.

In IHTP in general, one seeks to estimate unknown functions or parameters, for example unknown flow conditions or physical parameters of the material, from indirect measurements of the state, that is of the temperature field, which more often than not, in practical cases is

*Corresponding author: aciarbonetti@santafe-conicet.gov.ar

†sergio@cimne.upc.edu

‡rspies@santafe-conicet.gov.ar

contaminated by noise and/or can be acquired only at a few discrete points over the domain under study.

One of the engineering branches that has aroused the greatest interest in IHTP is electronic engineering, where thermal dissipation problems inside equipments or components are usually studied. These types of problems are generally associated with thermal conduction processes (see [15], [16]). This, like other growing branches in the last two decades, have generated a genuine interest in deepening the study of the thermal problems associated with the design of materials and thermal devices, seeking new material design methodologies, as well as efficient and cost-effective solutions.

Different methodological approaches to deal with the problem of designing thermal materials and devices in heterogeneous media having their roots in mathematical modeling, numerical solutions and computational mechanics have recently emerged. Among them, perhaps the most widely known is the computational design of thermal materials in heterogeneous media. This methodology arises from the application of optimization methods which were originally designed for solving solid mechanics problems ([4], [25]). Although this technique has shown to yield reasonable results (see for instance [10], [23], [9]), it has some severe drawbacks both in regard to the uniqueness of solutions (which appears to be highly dependent on the set of parameters used in the optimizing algorithm), as well as from the post-processing requirements of the obtained results.

Taking as inspirational base the optimization methods approach, we propose to tackle the problem of design of thermal materials in heterogeneous media by embedding it within the IHTP framework.

Undoubtedly the largest difficulty in dealing with IHTP problems is the fact that they are severely ill-conditioned which is a direct consequence of the violation of Hadamard's third postulate ([11]): lack of continuous dependence of the true solution on the data. Quite often there are additional complications coming from the lack of good measurements of the temperature field or the fact they are only available at a few scarce points. That makes extremely difficult to obtain good estimates of the heat flow which is generally needed for solving most IHTP.

Several variational models widely used for the numerical solution of IHTP generally introduce simplification hypotheses on the constitutive models and/or on the boundary conditions. For example in [32], the authors consider conductivity to be a polynomial form of the temperature. Similarly in [22], the model used for the IHTP problem assumes a linear dependence between conductivity and temperature. Although these simplifying hypotheses allow the successful implementation of conventional schemes for obtaining good numerical solutions, they are far from reflecting most real world problems.

In our case, the IHTP is associated with identifying an unrestricted heterogeneous conductivity profile in two dimensions from measurements of the temperature in a steady-state regime. From the materials design approach, an arbitrary field of temperatures and boundary conditions can be initially imposed so that they be consistent with the constraints of the expected design solution.

Heterogeneity adds a considerable degree of difficulty to an IHTP, however, that assumption corresponds to the problems of greatest practical interest, both in the analysis of thermographic images as in the material design problem in which we focus this contribution.

Implementation and numerical resolution of any IHTP will, at some point, require solving an optimization problem combined with some type of regularization to deal with ill-posedness.

In [14] the authors deal with the problem of identifying the conductivity profile from the temperature map. A simplifying assumption consisting of a direct dependence on conductivity and temperature is made together with pure Neumann-type boundary conditions. Under these hypotheses the authors solve the problem using a conjugate gradient approach. A similar

approach using conjugate gradient is used in [26] where the authors solve the inverse problem of finding the geometry of a defect or inclusion from an IR image.

In this work, a novel approach for solving the identification of an heterogeneous conductivity profile based on a variational approach of the PDE model followed by appropriate discretization and regularization is introduced. The model allows for mixed Dirichlet-Neumann boundary conditions, and no restrictive assumptions are made on the conductivity profile. The approach is numerically tested with 2D examples although the setting is not restricted to two dimensions.

1.1 A brief historical mathematical tracking of the problem

In this article we consider the problem of determining the elliptic coefficient profile function in an homogeneous elliptic boundary value problem.

Several authors have worked on this type of problems before, as they appear in several areas and concrete applied problems such as electrical conductivity problems, oil reservoir and ground water flow problems ([3], [5], [17], [19], [31]) among others.

In a 1980 article ([7]), A. P. Calderón considered the following problem. Let $\Omega \subset \mathbb{R}^n$, $n \geq 2$ be a bounded domain with Lipschitz boundary $\partial\Omega$ and define

$$L_{>0}^\infty(\Omega) \doteq \{k \in L^\infty(\Omega) : \exists \epsilon > 0 \text{ such that } k(x) \geq \epsilon > 0, \forall x \in \Omega\}. \quad (1)$$

Further, for $k \in L_{>0}^\infty(\Omega)$ let L_k be the differential operator

$$L_k(u) = \nabla \cdot (k \nabla u), \quad (2)$$

with domain $D(L_k) \doteq H^1(\Omega)$ and the quadratic form $Q_k : D(Q_k) \subset L_\infty(\partial\Omega) \rightarrow \mathbb{R}_0^+$, defined by the Dirichlet integral

$$Q_k(\varphi) = \int_\Omega k(x) (\nabla u_\varphi(x))^2 dx = \int_{\partial\Omega} \varphi(x) k(x) \frac{\partial u_\varphi}{\partial \nu} ds, \quad (3)$$

where ν denotes the outward normal to $\partial\Omega$ and $u_\varphi \in H^1(\Omega)$ is the solution of the Dirichlet boundary value problem

$$\begin{cases} L_k(u) = 0, & x \in \Omega, \\ u = \varphi, & x \in \partial\Omega. \end{cases} \quad (4)$$

It is timely to mention here that for φ in the space of traces of functions of $H^1(\Omega)$, the IBVP (4) has in fact a unique solution $u \in H^1(\Omega)$ (see [27]).

The problem considered by Calderón was to decide whether the function k is uniquely determined by the quadratic form Q_k and, if that is true, try to compute k in terms of Q_k . He was able to show that, with an appropriate norm defined in the space of quadratic forms, the mapping

$$M : k \longrightarrow Q_k \quad (5)$$

is bounded and analytic in $L_{>0}^\infty(\Omega)$. Moreover, although the general problem escaped its proof at that time, Calderón was able to show that for the linearized problem, the answer is affirmative, that is, $dM|_{k=const.}$ is an injective mapping. In addition he showed that if the function k is “close enough” to being a constant, then k is “nearly” determined by its quadratic form Q_k and derived a bound for the L^∞ -norm of the error (see [7] for details).

The previous result for “nearly constant” functions was later extended and formalized by Sylvester and Uhlmann ([28]) only for the case $n = 2$.

In 1984, Kohn and Vogelius ([18]) showed that if k is real analytic, then it can be uniquely determined from the knowledge of its Dirichlet integral Q_k . This result was later extended to piecewise real analytic functions k in 1985 by the same authors ([20]).

In 1987, Sylvester and Uhlmann ([29]) showed that for functions k sufficiently smooth, the quadratic form Q_k does indeed uniquely determine the function k . More precisely, they showed that the mapping M in (5) is injective over $C^\infty(\bar{\Omega}) \cap L^\infty_{>0}(\Omega)$.

The case of determining k in (4) from information about u on the whole domain Ω was studied by several authors. It is clear that some assumptions on k and/or on u must be required. Thus, for instance, it is evident that k cannot be uniquely determined in any subregion of Ω where $\nabla u = 0$. However, if $|\nabla u| > 0$ everywhere on Ω , once the values of k are given on a hypersurface transversal to ∇u , the method of characteristics will yield a unique solution. Several authors obtained similar uniqueness results under weaker assumptions on ∇u under diverse assumptions on k (e.g. [1], [2], [6], [24]).

There are several articles devoted to the problem of recovering k from information about u . However all of them assume some degree of smoothness on k (at least differentiability), which is almost never true in practical applications, where at best, only piecewise smoothness and jump discontinuities are to be expected, and quite often the available data consists only of noisy measurements at some discrete points. Although the mathematical theory of elliptic equations with discontinuous principal coefficients is well known ([27], [21]), there is not much done on the inverse problem of recovering k in these cases.

In this article we develop a method for approximating the perhaps discontinuous principal coefficient function based on a regularized variational approach. This approach takes appropriate care of the strong ill-posedness of the inverse problem which has been already carefully reported by several authors (see for instance [30], [8]), and is characteristic in all inverse heat conduction problems. Several numerical examples are presented that show that the method is able to yield very good approximations of k even in the case of discontinuous profiles.

2 Methodology

2.1 Preliminaries

Let $\Omega \subset \mathbb{R}^n$ ($n \geq 2$) a bounded open set with smooth boundary $\Gamma = \partial\Omega = \bar{\Gamma}_1 \cup \bar{\Gamma}_N$, with $\Gamma_1 \cap \Gamma_N = \emptyset$, $c, k, f, g, h \in L^2(\Omega)$ with $0 < \gamma_1 \leq k(x) \leq \gamma_2$ and $c \geq 0$, and consider the following problem, as described in Figure 1:

$$\mathcal{P} = \mathcal{P}(k, c, f, g, h) : \begin{cases} -\operatorname{div}(k(x)\nabla u(x)) + c(x)u(x) = f(x), & x \in \Omega, & (a) \\ u(x) = g(x), & x \in \Gamma_D, & (b) \\ k(x)\nabla u(x) \cdot \vec{n} = h(x), & x \in \Gamma_N. & (c) \end{cases} \quad (6)$$

Assume further that $g \in C(\Gamma_D)$ and define the affine subset of $H^1(\Omega)$

$$H_{\Gamma_D, g}^1(\Omega) = \{v \in H^1(\Omega) : v|_{\Gamma_D} = g\} \quad (7)$$

Multiplying equation (a) in (6) by $v \in H_{\Gamma_D, 0}^1(\Omega)$ and integrating we obtain:

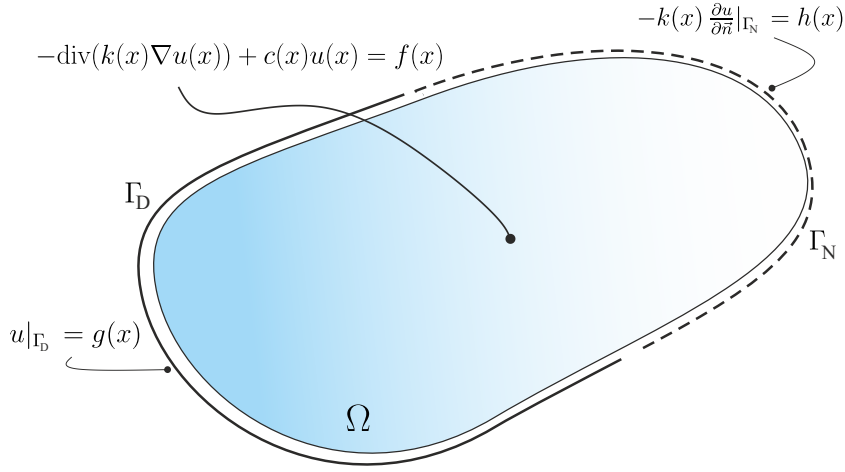


Figure 1: Schematic representation of problem $\mathcal{P}(k, c, f, g, h)$

$$\begin{aligned}
0 &= - \int_{\Omega} \operatorname{div}(k \nabla u) v \, dx + \int_{\Omega} c u v \, dx - \int_{\Omega} f v \, dx \\
&= \int_{\Omega} \langle k \nabla u, \nabla v \rangle \, dx - \int_{\partial \Omega} \langle k \nabla u, \vec{n} \rangle v \, ds + \int_{\Omega} c u v \, dx - \int_{\Omega} f v \, dx \\
&= \int_{\Omega} (\langle k \nabla u, \nabla v \rangle + c u v) \, dx - \int_{\Omega} f v \, dx - \int_{\Gamma_D \cup \Gamma_N} \langle k \nabla u, \vec{n} \rangle v \, ds \\
&= \int_{\Omega} (\langle k \nabla u, \nabla v \rangle + c u v) \, dx - \int_{\Omega} f v \, dx \\
&\quad - \int_{\Gamma_N} h v \, ds \quad (\text{since } v|_{\Gamma_D} = 0 \text{ and } k \nabla u \cdot \vec{n}|_{\Gamma_N} = h) \\
&\doteq F(u, v),
\end{aligned}$$

where $\langle \cdot, \cdot \rangle$ denotes the usual inner product in $L^2(\Omega)$ and \vec{n} is the outer normal to $\partial \Omega$. Hence, the variational formulation of problem \mathcal{P} is the following.

$VF(\mathcal{P})$: Find u in $H_{\Gamma_D, g}^1(\Omega)$ such that $F(u, v) = 0$ for all $v \in H_{\Gamma_D, 0}^1(\Omega)$, i.e. such that

$$\int_{\Omega} (\langle k \nabla u, \nabla v \rangle + c u v) \, dx = \int_{\Omega} f v \, dx + \int_{\Gamma_N} h v \, ds, \quad \forall v \in H_{\Gamma_D, 0}^1(\Omega). \quad (8)$$

Now define the continuous symmetric bilinear form $B_{k,c} : H^1(\Omega) \times H^1(\Omega) \rightarrow \mathbb{R}$ by

$$B_{k,c}(u, v) \doteq \int_{\Omega} (\langle k \nabla u, \nabla v \rangle + c u v) \, dx. \quad (9)$$

Then, if $c > 0$, $B_{k,c}$ defines an inner product on $H^1(\Omega)$ (note also that if $c > 0$ then $B_{k,c}$ is $H^1(\Omega)$ -elliptic) with associated norm

$$\|u\|_{B_{k,c}}^2 \doteq \int_{\Omega} (k \|\nabla u\|^2 + c |u|^2) \, dx. \quad (10)$$

Define also the energy functional $J : H_{\Gamma_D, g}^1(\Omega) \rightarrow \mathbb{R}$ by

$$\begin{aligned}
J(v) &\doteq \frac{1}{2} B_{k,c}(v, v) - \int_{\Omega} f v \, dx - \int_{\Gamma_N} h v \, ds \\
&= \frac{1}{2} \int_{\Omega} (\langle k \nabla v, \nabla v \rangle + c v^2) \, dx - \int_{\Omega} f v \, dx - \int_{\Gamma_N} h v \, ds.
\end{aligned} \quad (11)$$

In the next result we show that the directional derivatives of this energy functional are characterized by the functional F defined above.

Lemma 2.1. *For any $u \in H_{\Gamma_D, g}^1(\Omega)$ and any $v \in H_{\Gamma_D, 0}^1(\Omega)$ there holds*

$$\frac{d}{dt}J(u + tv)|_{t=0} = F(u, v).$$

Proof. First note that if $u \in H_{\Gamma_D, g}^1(\Omega)$ and $v \in H_{\Gamma_D, 0}^1(\Omega)$ then $u + tv \in H_{\Gamma_D, g}^1(\Omega)$ for all $t \in \mathbb{R}$. Moreover, $J(u + tv)$ is clearly differentiable with respect to t and

$$\begin{aligned} \frac{d}{dt}J(u + tv) &= \frac{d}{dt} \left[\frac{1}{2}B_{k,c}(u + tv, u + tv) - \int_{\Omega} (u + tv) f \, dx - \int_{\Gamma_N} (u + tv) h \, ds \right] \\ &= \frac{d}{dt} \left[\frac{1}{2} \int_{\Omega} (\langle k \nabla(u + tv), \nabla(u + tv) \rangle + c(u + tv)^2) \, dx - \int_{\Omega} f u \, dx \right. \\ &\quad \left. - t \int_{\Omega} f v \, dx - \int_{\Gamma_N} h u \, ds - t \int_{\Gamma_N} h v \, ds \right] \\ &= \int_{\Omega} (\langle k \nabla u, \nabla v \rangle + kt |\nabla v|^2 + cuv + tv^2) \, dx \\ &\quad - \int_{\Omega} f v \, dx - \int_{\Gamma_N} h v \, ds. \end{aligned} \tag{12}$$

Hence

$$\begin{aligned} \frac{d}{dt}J(u + tv)|_{t=0} &= \int_{\Omega} (\langle k \nabla u, \nabla v \rangle + cuv) \, dx - \int_{\Omega} f v \, dx - \int_{\Gamma_N} h v \, ds \\ &= F(u, v). \end{aligned} \tag{13}$$

□

The next theorem constitutes a fundamental result for the approximation framework that we shall develop later. It relates the solution of the variational problem $VF(\mathcal{P})$ with the minimizer of the energy functional J .

Theorem 2.2. *The variational formulation problem $VF(\mathcal{P})$ in (8) does have a unique solution u^* in $H_{\Gamma_D, g}^1(\Omega)$. Moreover, such a solution is characterized by the unique minimizer of the energy functional J defined in (11), i.e.*

$$u^* = \arg \min_{u \in H_{\Gamma_D, g}^1(\Omega)} J(u). \tag{14}$$

Proof. It is easy to show that the energy functional J in (11) is strictly convex and coercive over $H_{\Gamma_D, g}^1(\Omega)$ (for this we need c to be strictly positive), which implies the existence and uniqueness of a global minimizer $u^* \in H_{\Gamma_D, g}^1(\Omega)$. Hence, for any $v \in H_{\Gamma_D, 0}^1(\Omega)$ there must hold

$$0 = \frac{d}{dt}J(u^* + tv)|_{t=0} = F(u^*, v),$$

where the last equality follows from Lemma 2.1. Thus $F(u^*, v) = 0$ for all $v \in H_{\Gamma_D, 0}^1(\Omega)$ which implies that

$$\int_{\Omega} (\langle k \nabla u^*, \nabla v \rangle + cu^*v) \, dx = \int_{\Omega} f v \, dx + \int_{\Gamma_N} h v \, ds \quad \forall v \in H_{\Gamma_D, 0}^1(\Omega),$$

and therefore u^* is a solution of problem $VF(\mathcal{P})$ given in (8).

Now let us prove that the solution of problem $VF(\mathcal{P})$ is unique. Let u^* be a solution of problem $VF(\mathcal{P})$ and $w \in H_{\Gamma_D, g}^1(\Omega)$ be arbitrary. Then

$$\begin{aligned}
J(w) - J(u^*) &= \frac{1}{2}B_{k,c}(w, w) - \int_{\Omega} fw \, dx - \int_{\Gamma_N} hw \, ds - \frac{1}{2}B_{k,c}(u^*, u^*) \\
&\quad + \int_{\Omega} fu^* \, dx + \int_{\Gamma_N} hu^* \, ds \\
&= \frac{1}{2}(B_{k,c}(w, w) - B_{k,c}(u^*, u^*)) - \left(\int_{\Omega} \underbrace{f(w - u^*)}_{\in H_{\Gamma_D, 0}^1(\Omega)} \, dx + \int_{\Gamma_N} \underbrace{h(w - u^*)}_{\in H_{\Gamma_D, 0}^1(\Omega)} \, ds \right) \\
&= \frac{1}{2}(B_{k,c}(w, w) - B_{k,c}(u^*, u^*)) \\
&\quad - \int_{\Omega} (\langle k \nabla u^*, \nabla(w - u^*) \rangle + cu^*(w - u^*)) \, dx \quad (\text{since } u^* \text{ solves } VF(\mathcal{P})) \\
&= \frac{1}{2}(B_{k,c}(w, w) - B_{k,c}(u^*, u^*)) - B_{k,c}(u^*, w - u^*) \\
&= \frac{1}{2}B_{k,c}(w, w) - \frac{1}{2}B_{k,c}(u^*, u^*) - B_{k,c}(u^*, w) + B_{k,c}(u^*, u^*) \\
&= \frac{1}{2}(B_{k,c}(w, w) + B_{k,c}(u^*, u^*) - 2B_{k,c}(u^*, w)) \\
&= \frac{1}{2}B_{k,c}(w - u^*, w - u^*) \\
&= \frac{1}{2}\|w - u^*\|_{B_{k,c}}^2.
\end{aligned}$$

It then follows that $J(w) \geq J(u^*)$ for all $w \in H_{\Gamma_D, g}^1(\Omega)$ and $J(w) = J(u^*)$ if and only if $w = u^*$.

Hence problem $VF(\mathcal{P})$ has a unique solution $u^* \in H_{\Gamma_D, g}^1(\Omega)$ which is the unique minimizer of the energy functional $J(\cdot)$ over $H_{\Gamma_D, g}^1(\Omega)$. \square

Remark 2.1. *Note that within this variational formulation, the condition $c > 0$ (strictly) is necessary for uniqueness.*

Remark 2.2. *The condition $k(x) \geq \gamma_1 > 0$ is strictly necessary for J to be accretive. The condition $k(x) \leq \gamma_2 < \infty$ can be replaced by $k(x)$ bounded above by a positive function in $L^1(\Omega)$.*

2.2 The inverse problem

Now, given all the model parameters Ω , Γ_D , Γ_N , c , f , g and h , and a prescribed temperature distribution $\hat{u} \in H_{\Gamma_D, g}^1(\Omega)$ we consider the problem of finding the corresponding distributed conductivity field $k(\cdot)$ such that $u^* = \hat{u}$. That is, we intend to “invert” problem $\mathcal{P} = \mathcal{P}(k, c, f, g, h)$ with respect to k .

For simplicity and clarity in the presentation of the numerical results only the 2D-case will be considered, i.e. we will take $n = 2$, and we will assume $f = h \equiv 0$. Thus given a prescribed temperature field $\hat{u}(x, y) \in H_{\Gamma_D, g}^1(\Omega)$ we want to find $k = k(x, y)$ such that \hat{u} be the unique solution of problem $\mathcal{P}(k, c, f, g, h)$. Then, according to Theorem 2.2, $k(x, y)$ must satisfy:

$$\begin{aligned}
0 &= \frac{d}{dt}J(\hat{u} + tv)|_{t=0} \\
&= \int_{\Omega} (\langle k \nabla \hat{u}, \nabla v \rangle + c\hat{u}v) \, dx \, dy, \quad \forall v \in H_{\Gamma_D, 0}^1(\Omega).
\end{aligned} \tag{15}$$

3 Implementation

3.1 Discretizing the optimality condition and regularization

Let Ω_i , $1 \leq i \leq L$, be a partition of Ω by open sets, i.e. such that $\Omega_i \subset \Omega$ is open for all i , $\cup_{i=1}^L \overline{\Omega_i} = \overline{\Omega}$ and $\Omega_i \cap \Omega_j = \emptyset$ if $i \neq j$. For each i let $(x_i, y_i) \in \Omega_i$ and for any function $q(x, y)$ defined on Ω let us denote with q_i the value of q at the point (x_i, y_i) , i.e. $q_i \doteq q(x_i, y_i)$. With this notation, equation (15) can then be approximated by

$$0 = \sum_{i=1}^L [k_i (\hat{u}_{x,i} v_{x,i} + \hat{u}_{y,i} v_{y,i}) + c_i \hat{u}_i v_i] m(\Omega_i), \quad \forall v \in H_{\Gamma_D,0}^1(\Omega), \quad (16)$$

where the subscripts x and y denote the respective partial derivatives and $m(\Omega_i)$ is the Lebesgue measure of Ω_i . Assuming that the partition is regular so that $m(\Omega_i)$ is constant, equation (16) is equivalent to

$$\sum_{i=1}^L k_i (\hat{u}_{x,i} v_{x,i} + \hat{u}_{y,i} v_{y,i}) = - \sum_{i=1}^L c_i \hat{u}_i v_i, \quad \forall v \in H_{\Gamma_D,0}^1(\Omega). \quad (17)$$

Consider now a finite, arbitrary set of functions

$$v^r \in H_{\Gamma_D,0}^1(\Omega), \quad 1 \leq r \leq R. \quad (18)$$

Then (17) implies that

$$\sum_{i=1}^L k_i (\hat{u}_{x,i} v_{x,i}^r + \hat{u}_{y,i} v_{y,i}^r) = - \sum_{i=1}^L c_i \hat{u}_i v_i^r, \quad \forall 1 \leq r \leq R. \quad (19)$$

By defining

$$a_{r\ell} \doteq \hat{u}_{x,\ell} v_{x,\ell}^r + \hat{u}_{y,\ell} v_{y,\ell}^r \quad \text{and} \quad f_r \doteq - \sum_{i=1}^L c_i \hat{u}_i v_i^r, \quad 1 \leq \ell \leq L, \quad 1 \leq r \leq R,$$

we can write (19) as follows:

$$\sum_{\ell=1}^L a_{r\ell} k_\ell = f_r, \quad \forall 1 \leq r \leq R. \quad (20)$$

Let now \mathbf{A} be an $R \times L$ -dimensional matrix, $K \in \mathbb{R}^L$ and $F \in \mathbb{R}^R$ whose elements are $a_{r\ell}$, k_ℓ and f_r , respectively. Then, equation (20) can be simply written in matrix form as:

$$\mathbf{A} K = F. \quad (21)$$

Note that we still need to impose the condition that all components of the vector K be bounded between the values γ_1 and γ_2 . In what follows the idea is to solve (21) in the least squares sense, weakly imposing this restriction through a penalizer.

With the above in mind we consider a generalized Tikhonov-Phillips functional of the form:

$$J_{\alpha,W}(K) \doteq \|\mathbf{A}K - F\|^2 + \alpha W(K), \quad (22)$$

where $\alpha > 0$ is a regularization parameter and the penalizer $W(K)$ must be appropriately constructed in such a way as to deter non-admissible values as well as any undesired property of the conductivity profile $k(x, y)$.

3.2 Assumptions for the numerical implementations

In what follows we take $\Omega = (0, 1) \times (0, 1)$ and the Dirichlet and Neumann boundaries are the vertical and horizontal boundaries of Ω , respectively, i.e. $\Gamma_D = \{0, 1\} \times (0, 1)$ and $\Gamma_N = (0, 1) \times \{0, 1\}$ (see Figure 2).

Also, for the numerical experiments that follow, the Dirichlet boundary conditions will be prescribed as $g(x) = T_1$ on $\{0\} \times (0, 1)$ and $g(x) = T_2$ on $\{1\} \times (0, 1)$ where T_1 and T_2 are prescribed constant temperature values, with $T_1 > T_2$. Furthermore, we shall assume that $k(x, y)$ can take only two possible values, say k_L and k_U , with $0 < k_L < k_U < \infty$. Physically this implies that only two different materials having those conductivities can be present in the domain Ω . Clearly this assumption is extremely important to design appropriate forms for $W(K)$. It is timely to mention however that all the previous formulation leading up to equations (21) and (22) only requires the assumption $k \in L_{>0}^\infty(\Omega)$.

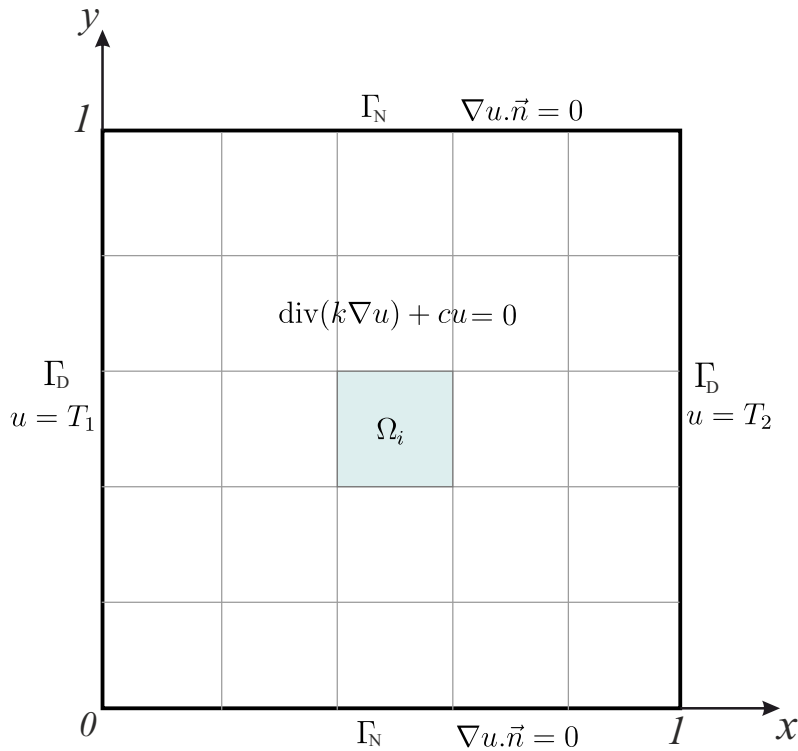


Figure 2: Schematic representation of the problem setting and its discretization

3.3 On the penalizer $W(\mathbf{K})$

Under the above assumption that at each point $(x, y) \in \Omega$, $k(x, y)$ can only take one of the values k_L or k_U , the penalizer $W(K)$ must be designed so that it deters each and every component of the vector K to take any but one of those two values. A simple way to do that is as follows.

Let $p : \mathbb{R} \rightarrow \mathbb{R}$ be the monic quadratic polynomial that vanishes at k_L and at k_U , i.e. $p(z) = (z - k_L)(z - k_U) = z^2 - (k_L + k_U)z + k_L k_U$. Next we define $W_1 : \mathbb{R}^L \rightarrow \mathbb{R}_0^+$ as

$$W_1(K) \doteq \|p(K)\|_{\mathbb{R}^L}^2, \quad (23)$$

where p acting on the vector K must be understood as its component-wise action, i.e. $(p(K))_i = p(K_i)$. Clearly, then, $W_1(K) \geq 0$ and $W_1(K) = 0$ if and only if each and every component of K takes one of the two values k_L or k_U .

A different approach is to design an ad-hoc penalizer which, besides promoting all the components of the vector K to take only the values k_L or k_U , provides data-driven information about where to take one or the other value. With that in mind let $b_U \in \mathbb{R}^L$ be a binary vector whose i^{th} component takes the value 1 if and only if the gradient of \hat{u} at the point (x_i, y_i) is “large”, i.e. if $\|\nabla \hat{u}(x_i, y_i)\| > \gamma$, where γ is a certain prescribed threshold value, and define the penalizer $W_2(K)$ as

$$W_2(K) \doteq \|b_U \odot (K - k_L \mathbf{1})\|^2, \quad (24)$$

where \odot denotes elementwise product and $\mathbf{1} \in \mathbb{R}^L$ is a vector of ones. Hence, at a point where $\|\nabla \hat{u}\|$ is large (as dictated by the threshold parameter γ), this penalizer will discourage the corresponding component of K to assume any value except k_L .

In the definitions (23) and (24), the \mathbb{R}^L -norm can be replaced by any other norm. Finally, many other options for the functional $W(K)$ exist if other restrictions on the function $k(x, y)$ are to be enforced, for instance, certain regularity properties (which clearly would not be appropriate for our case at hand).

3.4 Examples, numerical experiments and discussions

3.4.1 Case I

We first solved the forward problem \mathcal{P} under the previous assumptions with $T_1 = 322.0$ [K], $T_2 = 283.0$ [K], $c(x, y) = 1.0 = \text{constant}$, and $k(x, y)$ as shown in Figure 3. For this we used a standard discretization by finite element method, using biquadratic interpolation elements S2 with 8-nodes for computing $\hat{u}(x, y)$, $\hat{u}_x(x, y)$ and $\hat{u}_y(x, y)$. The same scheme was used to solve all forward problems in the coming cases. The resulting temperature distribution $\hat{u}(x, y)$, whose discretized values are then used as inputs for the inverse problem, is shown in Figure 4 b).

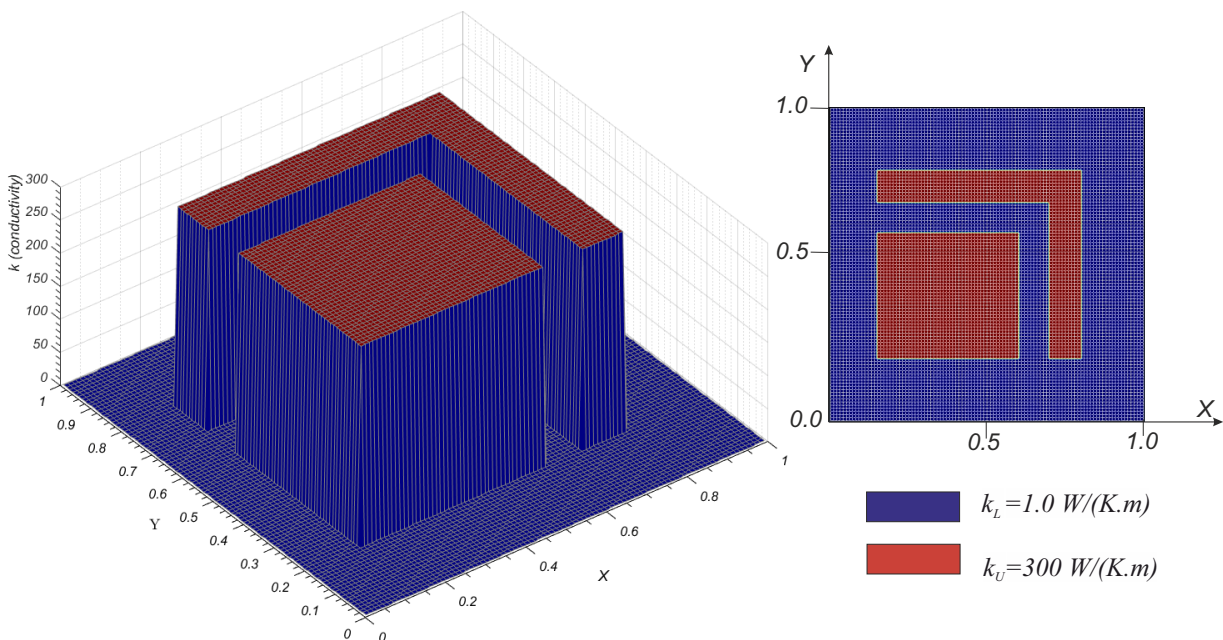


Figure 3: Conductivity $k(x, y)$ used for solving the forward problem in Case I

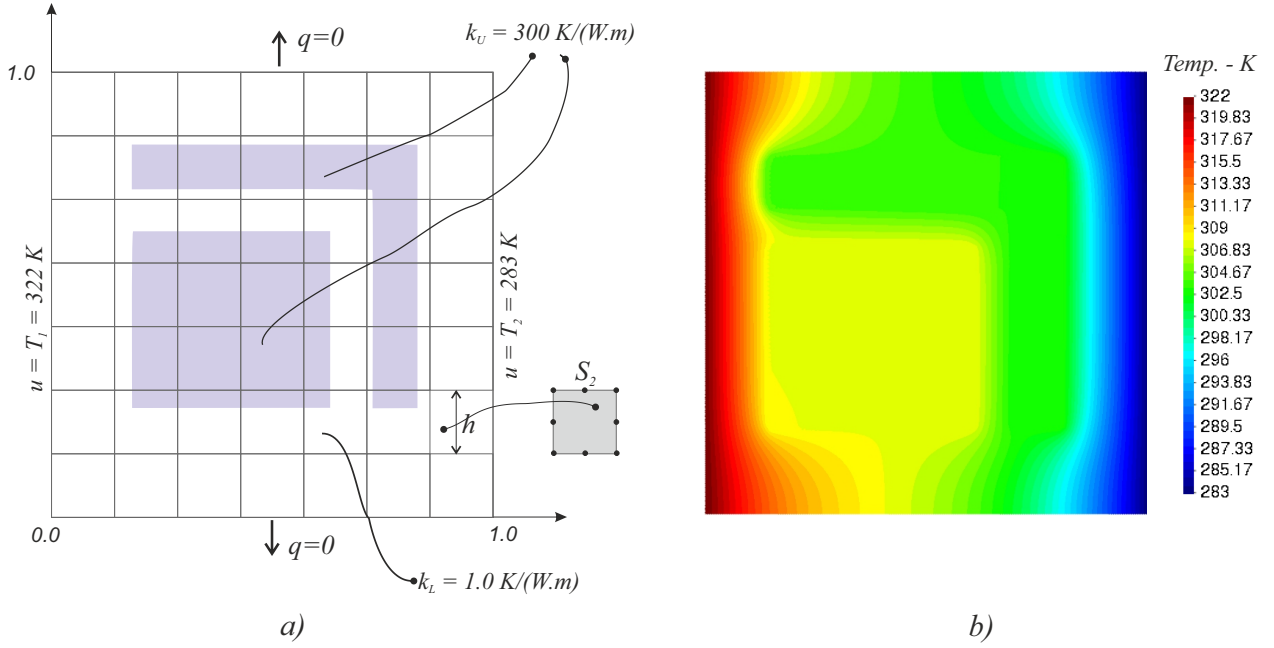


Figure 4: a) Sketch of the discretized domain used to solve the forward problem, for case I. The finite element mesh S_2 used is regular with elements size $h = 1/200$. b) Temperature distribution $\hat{u}(x, y)$ for $k(x, y)$ as in Figure 3.

Setting 1: For this case we picked $\alpha = 0$ (non-penalized case) in (22) and the set of functions $v^r \in H_{\Gamma_D, 0}^1(\Omega)$, $1 \leq r \leq R$, was chosen as an appropriate single index reordering of the set of functions:

$$v^{m,n}(x, y) \doteq x^m(1-x)^n, \quad \text{for } 1 \leq m, n \leq M, \quad (25)$$

where $M \in \mathbb{N}$ is appropriately chosen. Note that $v^{m,n} \in H_{\Gamma_D, 0}^1(\Omega)$ as required in (15). Thus $R = M^2$ and $v_i^r \doteq v^{m,n}(x_i, y_i) = x_i^m(1-x_i)^n$ for all $1 \leq i \leq L$, $1 \leq r \leq R$ and $1 \leq m, n \leq M$. The general idea behind our approach is to somehow determine “how much” information about $k(x, y)$ can be obtained from the set of functions (25) as a subset of $H_{\Gamma_D, 0}^1(\Omega)$ through the optimality equation (15) which characterizes $k(x, y)$ or, more precisely, through its discrete counterpart (17).

We first solved (22) with $\alpha = 0$. Hence, no restrictions on $k(x, y)$ were imposed. Also, we used $M = 5$ in (25) which results in $R = 25$ test functions in (18). We computed the best approximate solution (i.e. the least squares solution of minimal norm) of $AK = F$ as $K^\dagger = A^\dagger F$ where A^\dagger denotes the Moore-Penrose generalized inverse of A ([8]). The obtained (discretized) $k(x, y)$ is plotted in Figure 5. We observe how the basic geometric distribution of the two possible values of $k(x, y)$ is already recovered using only the 25 functions $v^{m,n}(x, y)$ in (25) with $M = 5$, even without using any penalization in equation (22). It is timely to point out here that the severe ill-posedness of the problem is clearly reflected on the matrix A whose condition number turns out to be approximately equal to 2.5×10^{18} (here we used $L = 10^4$ resulting from a 100×100 regular grid on Ω). It is reasonable to think that a better restoration of $k(x, y)$ could be obtained by taking $\alpha > 0$ and minimizing the functional $J_{\alpha, W}$ given in (22) using the penalizer $W_1(K)$ defined in (23).

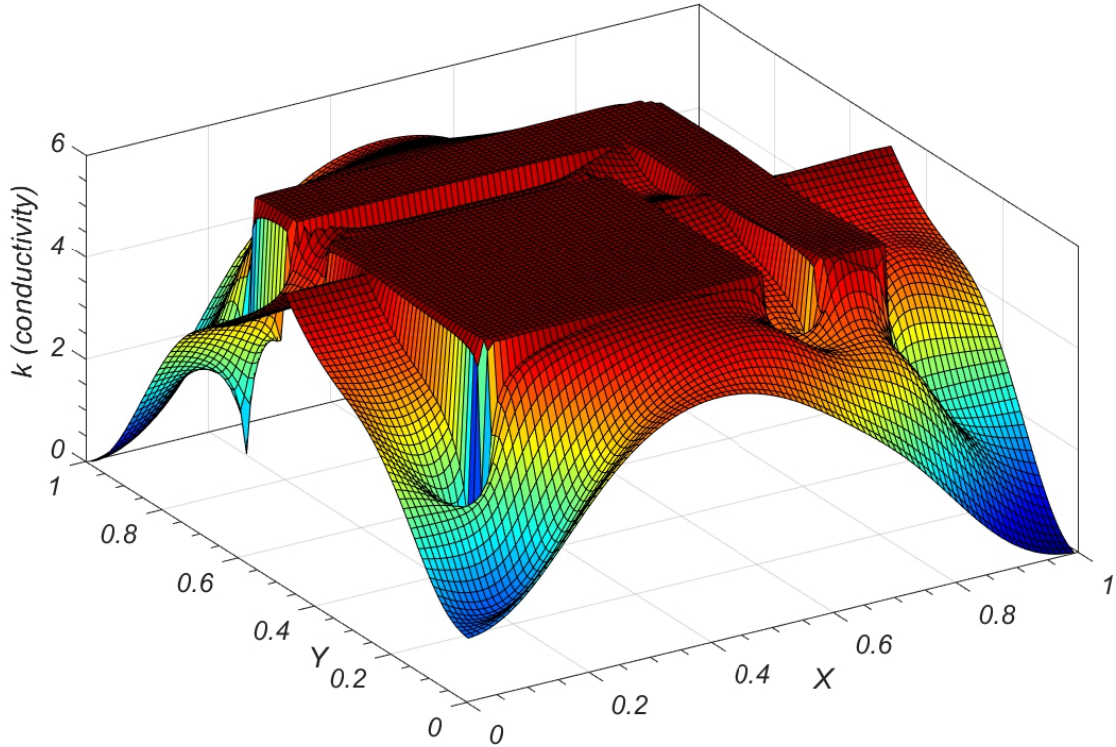


Figure 5: Reconstruction of $k(x, y)$ obtained using $\hat{u}(x, y)$ as in Figure 4, using a non-penalized least squares approach.

Setting 2: For this example all parameters and functions are the same as in Setting 1, except that here we used $\alpha > 0$ in (22) and the penalizer was chosen as $W(K) = W_1(K)$ given by (23). The appropriate value of $\alpha > 0$ was picked by means of the L-curve method ([13], [12], [8]). Note that finding the minimizer of (22) corresponds to finding the Tikhonov-Phillips W_1 -regularized solution of (21). The obtained conductivity $k(x, y)$ is shown in Figure 6. As it can be seen, the introduction of the penalizer W_1 , as expected, induces k to take only values around $K_L = 1.0$ and $K_U = 300$. Although the correct geometric profile of $k(x, y)$, shown in Figure 3, can be clearly appreciated in this figure, the obtained result is far from being satisfactory. It is highly desirable to come up with a better penalizer that be able to reconstruct the conductivity distribution as close as possible.

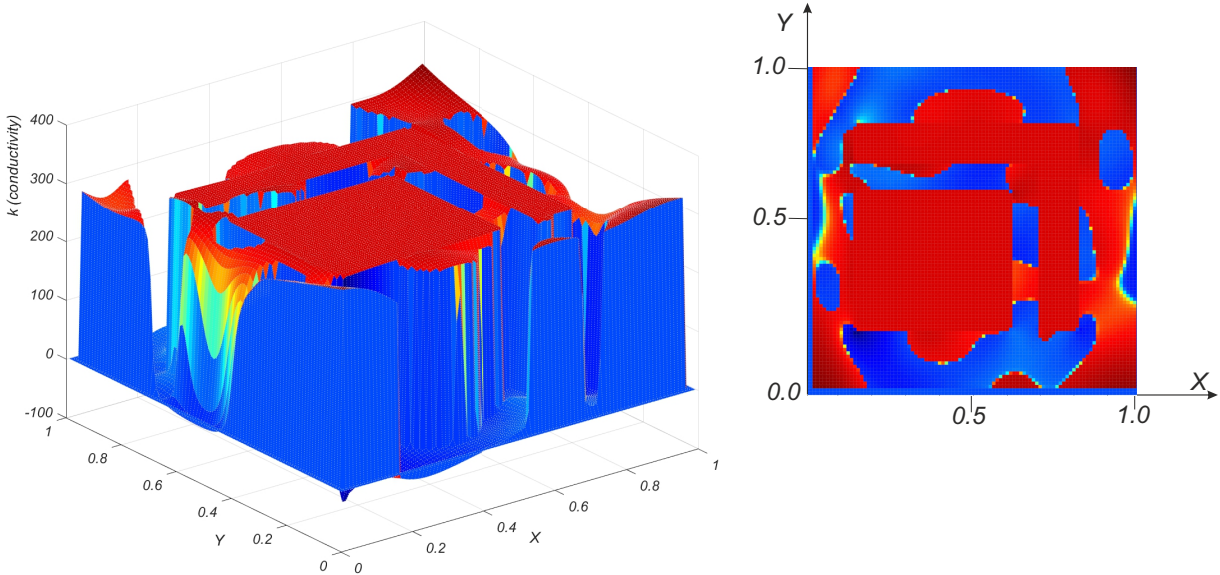


Figure 6: Reconstruction of $k(x, y)$ obtained using $\hat{u}(x, y)$ as in Figure 4, via the penalized least squares approach (22) with $W(K) = W_1(K)$ given as in (23).

Setting 3: Here we proceed to use the penalizer $W_2(K)$ which, unlike W_1 , includes data-driven information about the local size of $\|\nabla \hat{u}(x, y)\|$. Hence, $k(x, y)$ is now obtained as the Tikhonov-Phillips W_2 -regularized solution of problem (21), that is, as the global minimizer of (22) when the penalizer $W(K)$ is given by $W_2(K)$ as defined in (24). The value of the threshold parameter γ needed to define b_U in (24) was set to $0.01 * M$, where $M \doteq \max_{1 \leq i \leq L} \|\hat{u}(x_i, y_i)\|$ while the regularization parameter α was again chosen by means of the L-curve method. The restored conductivity profile $k(x, y)$ is shown in Figure 7. As it can be observed, although some small artifacts still appear, a much better approximation of the true profile is obtained.

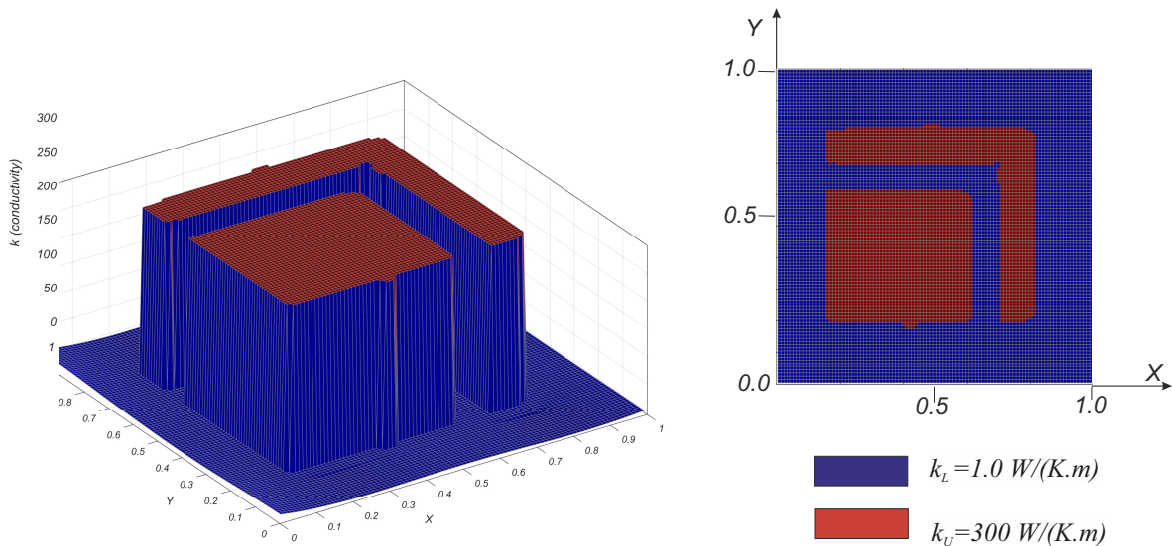


Figure 7: Reconstruction of $k(x, y)$ obtained using $\hat{u}(x, y)$ as in Figure 4, using a penalized least squares approach with $W(K) = W_2(K)$ defined as in (24)

We now proceed to present the results obtained for three other different configurations of

the conductivity profile $k(x, y)$. For the sake of brevity, we shall only show the results obtained under Setting 3 of Case I, which is clearly by far the best approach for solving the inverse problem at hand.

3.4.2 Case II

For this case the conductivity profile is as depicted in Figure 8. Here again we computed $\hat{u}(x, y)$ by first running the forward problem with $T_1 = 318.15 [K]$, $T_2 = 288.15 [K]$, $c(x, y) = 1.0 = \text{constant}$. The resulting temperature distribution $\hat{u}(x, y)$, whose discretized values are used as inputs for the inverse problem, is shown in Figure 9 b).

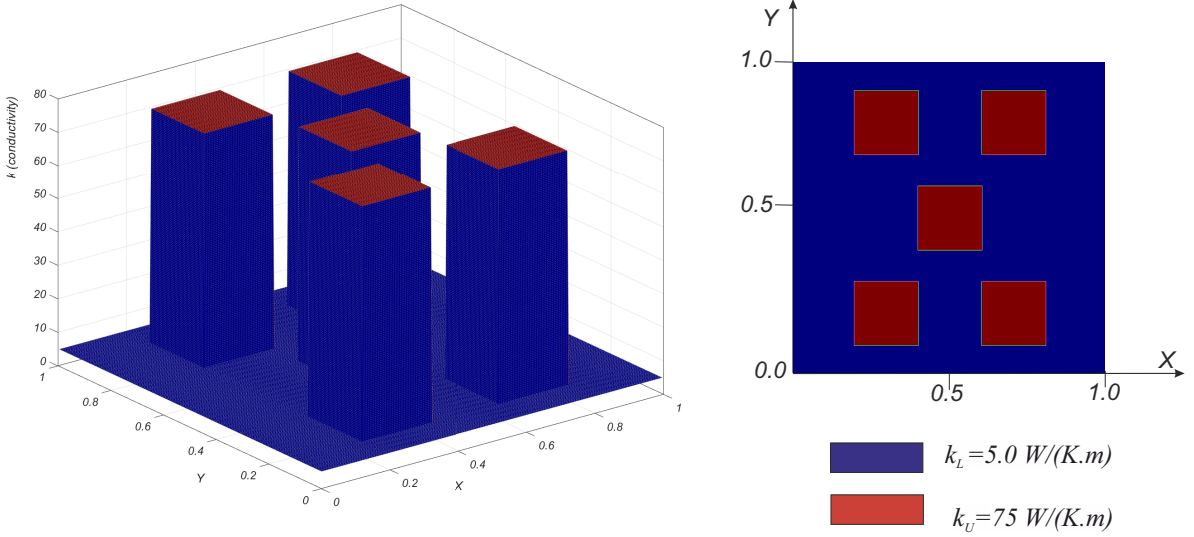


Figure 8: Distributed values of the conductivity $k(x, y)$ used for solving the forward problem in Case II

Here, the set of functions $v^r \in H_{\Gamma_D,0}^1(\Omega)$, $1 \leq r \leq R$, was chosen as in Setting 1 of Case I. We proceeded to compute the generalized Tikhonov-Phillips solution of problem (21) when the penalizer is given by $W_2(K)$ as defined in (24). The threshold parameter was now chosen as $\gamma = 0.0125 M$, where, as before, $M \doteq \max_{1 \leq i \leq L} \|\hat{u}(x_i, y_i)\|$ while the regularization parameter α was again chosen by means of the L-curve method. The restored conductivity profile $k(x, y)$ is shown in Figure 10. Here again, despite a few artifacts, we can observe how our method is able to satisfactory reconstruct the conductivity distribution profile.

3.4.3 Case III

For this case the conductivity profile is as depicted in Figure 11. Here again we computed $\hat{u}(x, y)$ by first running the forward problem with $T_1 = 373.15 [K]$, $T_2 = 353.15 [K]$, $c(x, y) = 1.0 = \text{constant}$, $k_U = 100$ and $k_L = 0.7$. The resulting temperature distribution $\hat{u}(x, y)$ is shown in Figure 12 b).

As in the previous case, the set of functions $v^r \in H_{\Gamma_D,0}^1(\Omega)$, $1 \leq r \leq R$, was chosen as in Setting 1 of Case I. We proceeded to compute the generalized Tikhonov-Phillips solution of problem (21) when the penalizer is given by $W_2(K)$ as defined in (24). The value of the threshold was now chosen as $\gamma = 0.0125 M$, where, as before, $M \doteq \max_{1 \leq i \leq L} \|\hat{u}(x_i, y_i)\|$ while

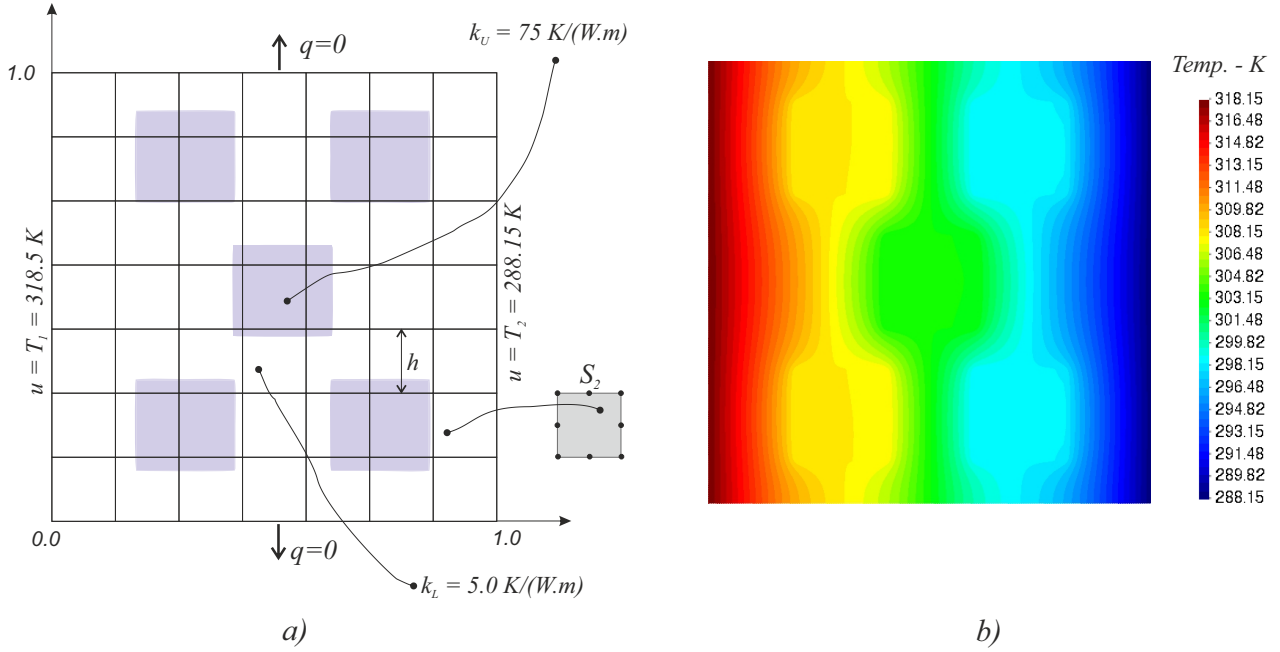


Figure 9: a) Sketch of the discretized domain used to solve the forward problem for Case II. The finite element mesh S_2 used is regular with elements size $h = 1/200$. b) Temperature distribution $\hat{u}(x, y)$ for $k(x, y)$ as in Figure 8, Case II.

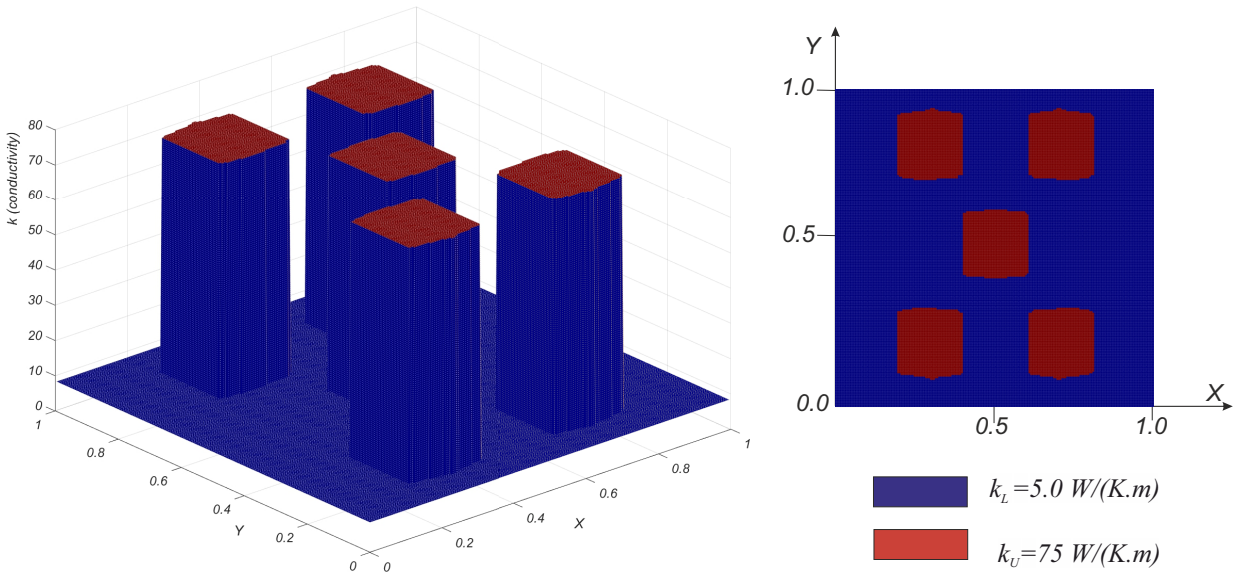


Figure 10: Reconstruction of $k(x, y)$ obtained using $\hat{u}(x, y)$ as in Figure 9, using a penalized least squares approach with $W_2(K)$ defined as in (24), Case II.

the regularization parameter was again chosen by means of the L-curve method. The restored conductivity profile $k(x, y)$ is shown in Figure 13. Once again we can observe how our method is able to satisfactory reconstruct the conductivity distribution profile.

3.4.4 Case IV

We end up presenting a case where the conductivity profile has a very irregular shape, as depicted in Figure 14. The goal is to verify if the methods is able to detect these irregular

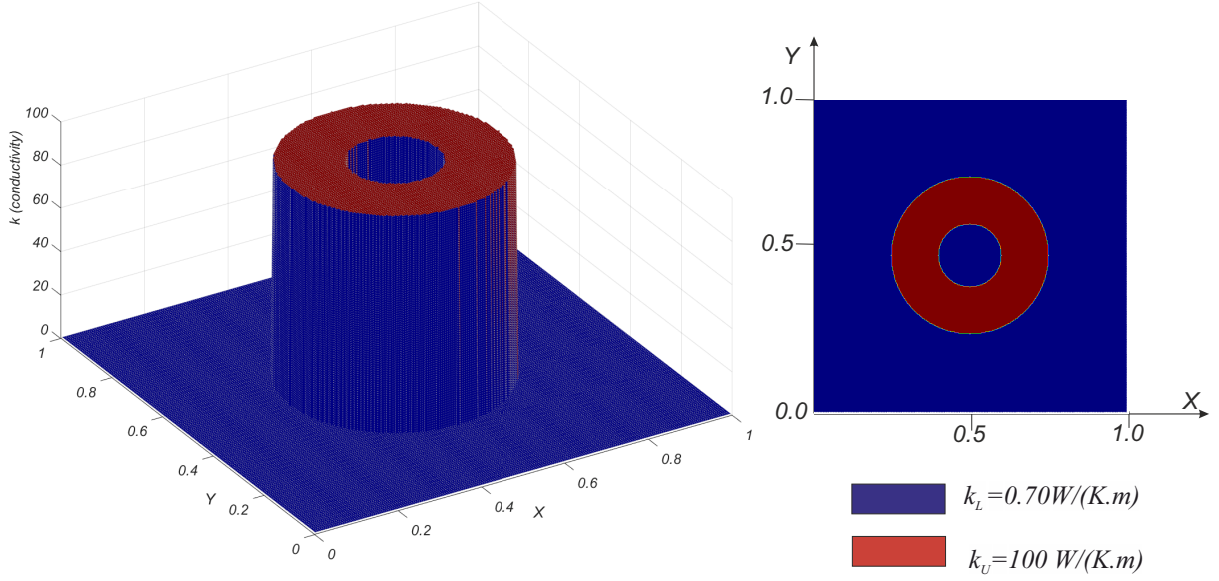


Figure 11: Distributed values of the conductivity $k(x, y)$ used for solving the forward problem in Case III

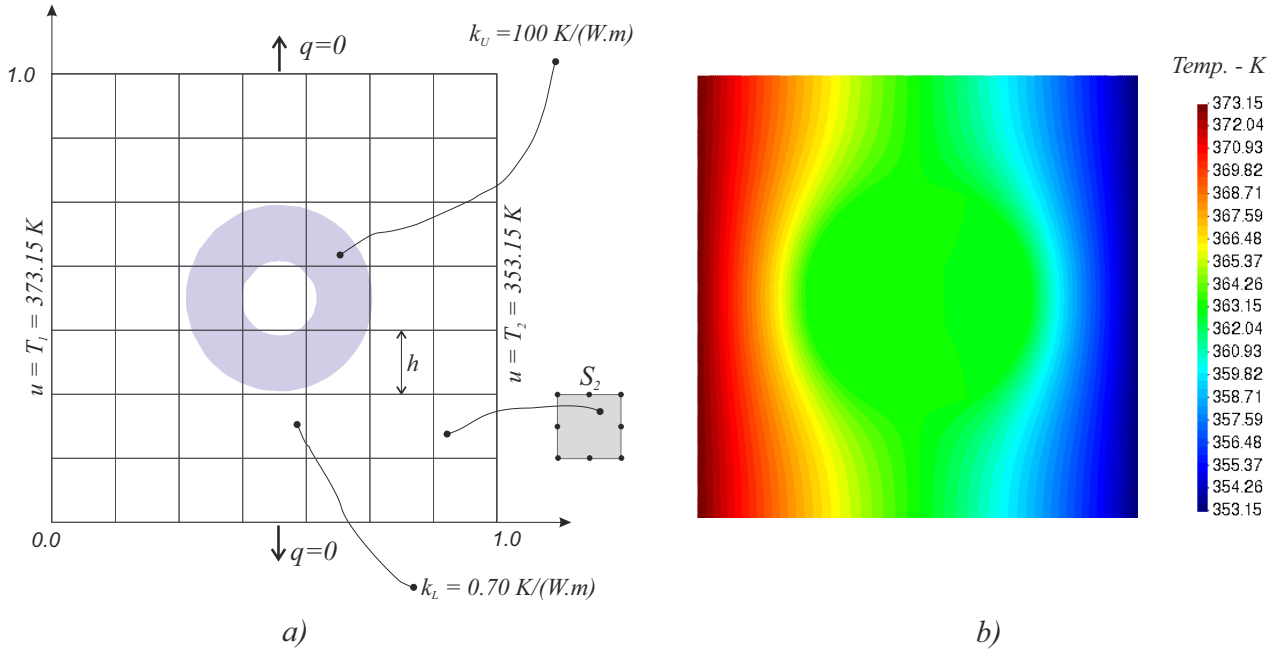


Figure 12: a) Sketch of the discretized domain used to solve the forward problem, for case III. The finite element mesh S_2 used is regular with elements size $h = 1/200$. b) Temperature distribution $\hat{u}(x, y)$ for $k(x, y)$ as in Figure 11, Case III.

boundaries in $k(x, y)$. Here again we computed $\hat{u}(x, y)$ by first running the forward problem with $T_1 = 308.15 [K]$, $T_2 = 298.15 [K]$, $c(x, y) = 1.0 = \text{constant}$, $k_U = 125$ and $k_L = 20$. The resulting temperature distribution $\hat{u}(x, y)$ is shown in Figure 15 b).

As in the previous cases, we proceeded to compute the generalized Tikhonov-Phillips solution of problem (21), as the global minimizer of (22) when the penalizer is given by $W_2(K)$ as defined in (24). The value of the threshold in this case was chosen as $\gamma = 0.3153 M$, with $M \doteq \max_{1 \leq i \leq L} \|\hat{u}(x_i, y_i)\|$ while the regularization parameter was again chosen by means of the L-curve method. The restored conductivity profile $k(x, y)$ is shown in Figure 16. Once

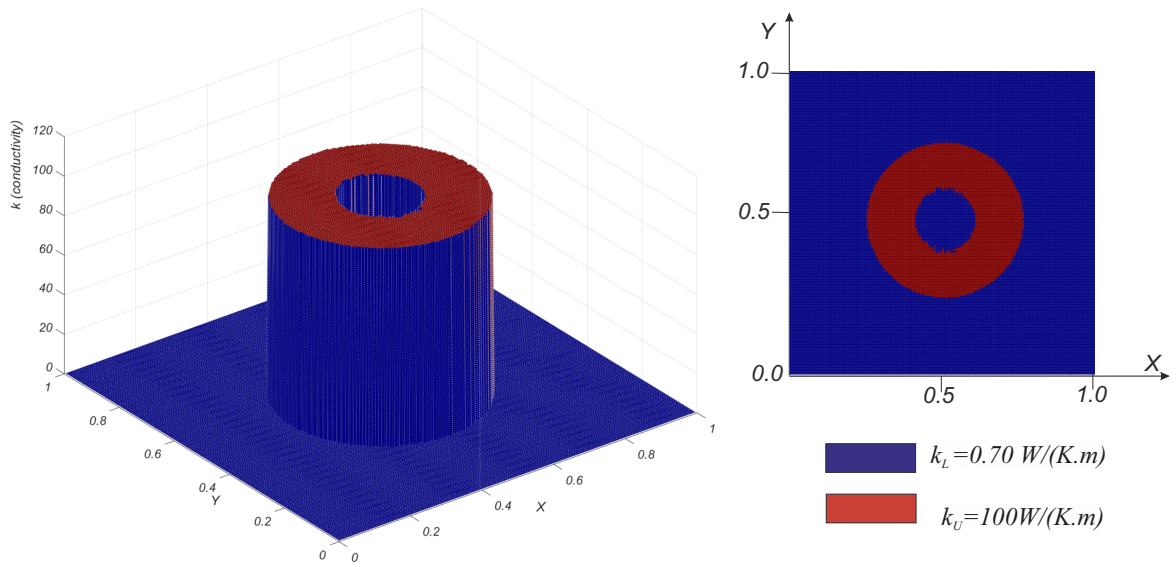


Figure 13: Reconstruction of $k(x, y)$ obtained using $\hat{u}(x, y)$ as in Figure 12 b), using a penalized least squares approach with $W_2(K)$ defined as in (24), Case III.

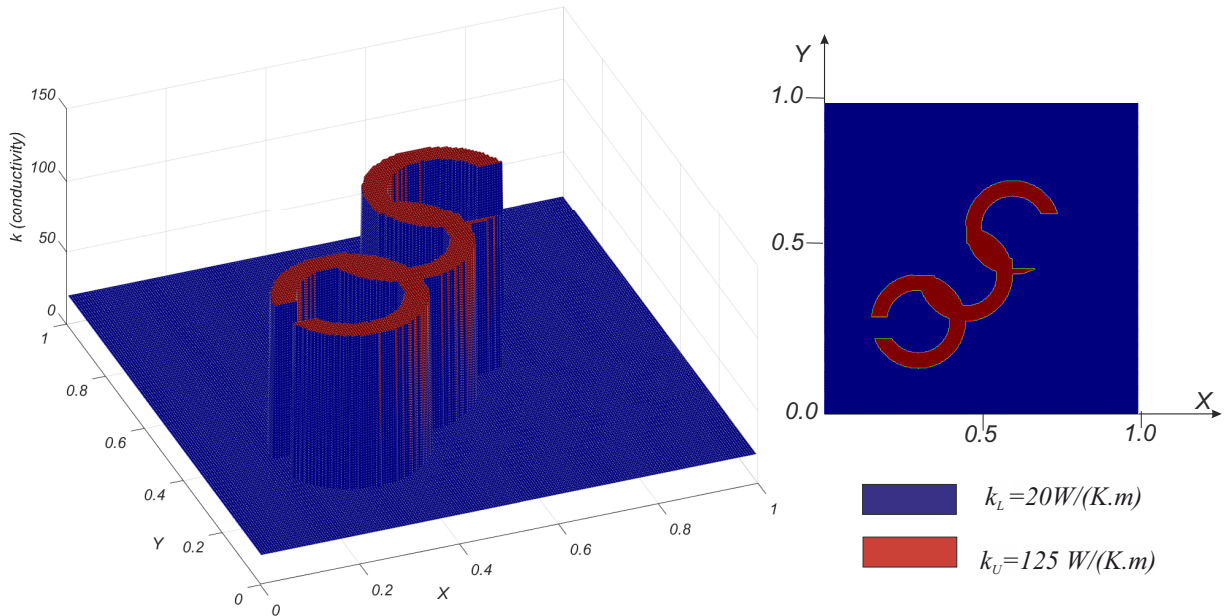


Figure 14: Distributed values of the conductivity $k(x, y)$ used for solving the forward problem in Case IV.

again, we can observe how our method is able to quite satisfactory reconstruct the conductivity distribution profile.

Conclusions and future work

In this article we introduced a method for solving the inverse problem of estimating the principal coefficient in a steady state elliptic diffusion equation. The method is based on the discretization of an optimality equation derived from a variational approach which leads to a least squares problem based on a fidelity term. The method is followed by regularization consisting of adding an appropriate penalizer, encoding prior-information about the conductivity profile, leading to a the problem of finding the minimizer of a generalized Tikhonov-Phillips functional.

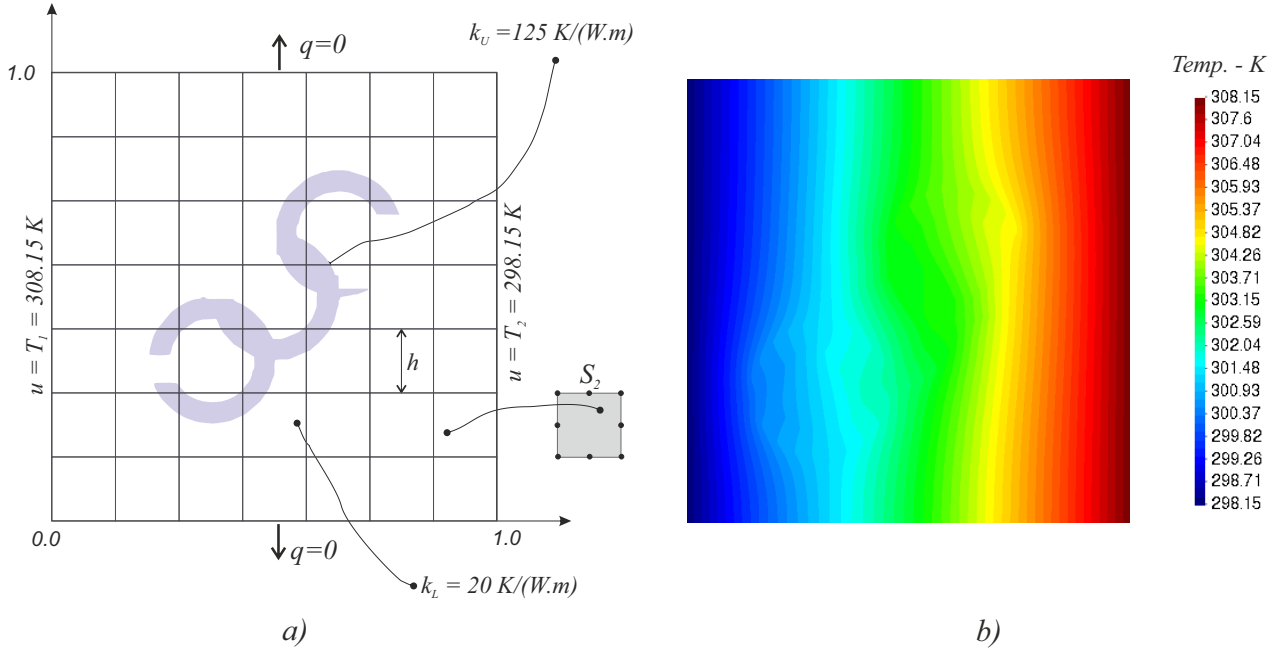


Figure 15: a) Sketch of the discretized domain used to solve the forward problem, for case IV. The finite element mesh S_2 used is regular with elements size $h = 1/200$. b) Temperature distribution $\hat{u}(x, y)$ for $k(x, y)$ as in Figure 14, Case IV.

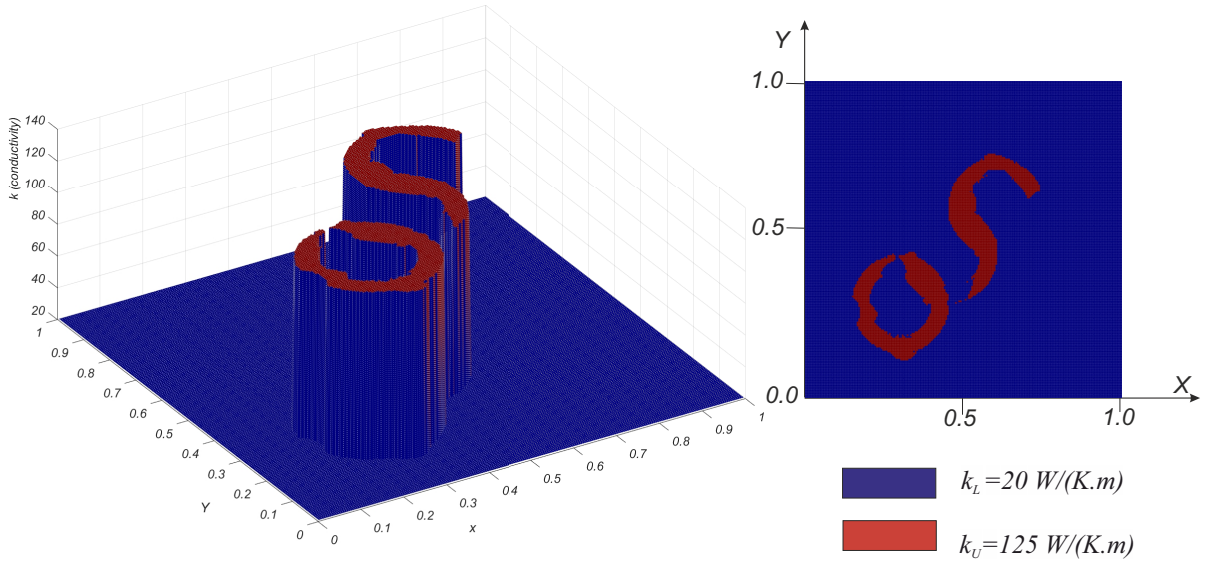


Figure 16: Reconstruction of $k(x, y)$ obtained using $\hat{u}(x, y)$ as in Figure 15, using a penalized least squares approach with $W_2(K)$ defined as in (24), Case IV.

Several numerical experiments with different types of discontinuous distributions for the leading coefficient function $k(x, y)$ were presented, showing that, with the appropriate penalizer, the method yields excellent reconstructions of the true (unknown in practical problems) function.

There is clearly much room for improvements and generalizations. First we find it timely to point out that several numerical experiments have shown that adding more functions in $H_{\Gamma_D,0}^1(\Omega)$ to the the set in (25) does not improve the reconstructions in none of the cases. That

is due to the severe ill-posedness of the problem.

As it was shown, the success of the method is highly dependent on the appropriate choice of the regularization term. The penalizer W_2 defined in (24) works very well for the case in which $k(x, y)$ takes only two prescribed values. However, in that case, although experiments showed that the results are somewhat robust with respect to the choice of γ , designing rigorous analytic ways for estimating an optimal value of that threshold parameter γ is highly desirable.

A detailed analysis of the results and images show that the small artifacts obtained in the reconstruction of the function $k(x, y)$ are always associated to places where $|\nabla u| = 0$. Although this is reasonable since at those points k cannot be restored, more research is necessary to come up with a way to avoid those artifacts, perhaps taking into account a-priori information about the expected conductivity.

In regard to the design of appropriate penalizers, no general recipe is expected to be found which will work for arbitrary functions $k(x, y)$. It is not completely clear, for instance, what would be a good choice for the penalizer $W(\cdot)$ in the case in which three (or more) possible conductivity values are present. Efforts in all of these directions are currently under way.

Acknowledgements

This work was supported in part by Consejo Nacional de Investigaciones Científicas y Técnicas, CONICET, through grants PIP 2021-2023 number 11220200100806CO and PUE-IMAL number 22920180100041CO, by Agencia Nacional de Promoción de la Investigación, el Desarrollo Tecnológico y la Innovación, through grant PICT-2019-2019-01933 and by Universidad Nacional del Litoral, through grant CAI+D 2020 Nro. 50620190100069LI.

References

- [1] G. Alessandrini. On the identification of the leading coefficient of an elliptic equation. *Pubblicazioni dell'Istituto di analisi globale e applicazioni.*, 1984.
- [2] G. Alessandrini. An identification problem for an elliptic equation in two variables. *Annali di Matematica pura ed applicata*, (145):265–295, 1986.
- [3] J. Bear. *Dynamics of Fluids in Porous Media*. American Elsevier, New York, 1972.
- [4] M. P. Bendsøe and O. Sigmund. *Topology optimization. Theory, methods, and applications*. Springer-Verlag, 2003.
- [5] F. Bongiorno and V. Valente. A method of characteristics for solving an underground water maps problem. *Pubblicazioni Istituto per le Applicazioni del Calcolo "Mauro Picone". III*, 116, 1977.
- [6] F. Bongiorno and V. Valente. *A Method of Characteristics for Solving an Underground Water Maps Problem*. Pubblicazioni (Istituto per le applicazioni del calcolo "Mauro Picone"). IAC, 1977.
- [7] A. P. Calderón. On an inverse boundary value problem. *Computational & Applied Mathematics*, 25:133 – 138, 00 2006.
- [8] H. W. Engl, M. Hanke, and A. Neubauer. *Regularization of inverse problems*, volume 375 of *Mathematics and its Applications*. Kluwer Academic Publishers Group, Dordrecht, 1996.

- [9] V. D. Fachinotti, Á. A. Ciarbonetti, I. Peralta, and I. Rintoul. Optimization-based design of easy-to-make devices for heat flux manipulation. *International Journal of Thermal Sciences*, 128:38–48, 2018.
- [10] V. D. Fachinotti, I. Peralta, A. E. Huespe, and A. A. Ciarbonetti. Control of heat flux using computationally designed metamaterials. In *EngOpt 2016 – 5th International Conference on Engineering Optimization*, Iguassu Falls, Brasil, 2016.
- [11] J. Hadamard. Sur les problèmes aux dérivées partielles et leur signification physique. *Princeton University Bulletin*, 13:49–52, 1902.
- [12] P. C. Hansen. *Discrete Inverse Problems: Insight and Algorithms*, volume FA07 of *Fundamentals of Algorithms*. Society for Industrial and Applied Mathematics, Philadelphia, 2010.
- [13] P. C. Hansen and D. P. O’Leary. The use of the L -curve in the regularization of discrete ill-posed problems. *SIAM J. Sci. Comput.*, 14(6):1487–1503, 1993.
- [14] C.-H. Huang and S.-C. Chin. A two-dimensional inverse problem in imaging the thermal conductivity of a non-homogeneous medium. *International Journal of Heat and Mass Transfer*, 43(22):4061–4071, 2000.
- [15] M. Janicki and A. Napieralski. Inverse heat conduction problems in electronics with special consideration of analytical analysis methods. In *2004 International Semiconductor Conference. CAS 2004 Proceedings (IEEE Cat. No.04TH8748)*, volume 2, pages 455–458 vol.2, 2004.
- [16] M. Janicki, M. Zubert, and A. Napieralski. Application of inverse heat conduction methods in temperature monitoring of integrated circuits. *Sensors and Actuators A: Physical*, 71(1):51–57, 1998.
- [17] I. Knowles and R. Wallace. A variational solution for the aquifer transmissivity problem. *Inverse Problems*, 12(6):953–963, dec 1996.
- [18] R. Kohn and M. Vogelius. Determining conductivity by boundary measurements. *Communications on Pure and Applied Mathematics*, 37(3):289–298, 1984.
- [19] R. V. Kohn and B. D. Lowe. A variational method for parameter identification. *ESAIM: Mathematical Modelling and Numerical Analysis*, 22(1):119–158, 1988.
- [20] R. V. Kohn and M. Vogelius. Determining conductivity by boundary measurements ii. interior results. *Communications on Pure and Applied Mathematics*, 38(5):643–667, 1985.
- [21] W. Littman, G. Stampacchia, and H. F. Weinberger. Regular points for elliptic equations with discontinuous coefficients. *Annali della Scuola Normale Superiore di Pisa-Classe di Scienze*, 17(1-2):43–77, 1963.
- [22] M. Mierzwiczak and J. Kołodziej. The determination temperature-dependent thermal conductivity as inverse steady heat conduction problem. *International Journal of Heat and Mass Transfer*, 54(4):790–796, 2011.
- [23] I. Peralta, V. D. Fachinotti, and Á. A. Ciarbonetti. Optimization-based design of a heat flux concentrator. *Scientific Reports*, 7(40591):1–8, 2017.
- [24] G. R. Richter. An inverse problem for the steady state diffusion equation. *SIAM Journal on Applied Mathematics*, 41(2):210–221, 1981.

- [25] H. Rodrigues, J. M. Guedes, and M. P. Bendsøe. Hierarchical optimization of material and structure. *Structural and Multidisciplinary Optimization*, 24(1):1–10, 2002.
- [26] F. L. Rodríguez and V. de Paulo Nicolau. Inverse heat transfer approach for ir image reconstruction: Application to thermal non-destructive evaluation. *Applied thermal engineering*, 33:109–118, 2012.
- [27] G. Stampacchia. Équations elliptiques du second ordre à coefficients discontinus. *Séminaire Jean Leray*, (3):1–77, 1963-1964.
- [28] J. Sylvester and G. Uhlmann. A uniqueness theorem for an inverse boundary value problem in electrical prospection. *Communications on Pure and Applied Mathematics*, 39(1):91–112, 1986.
- [29] J. Sylvester and G. Uhlmann. A global uniqueness theorem for an inverse boundary value problem. *Annals of Mathematics*, 125(1):153–169, 1987.
- [30] S. Yakowitz and L. Duckstein. Instability in aquifer identification: Theory and case studies. *Water Resources Research*, 16(6):1045–1064, 1980.
- [31] W. W.-G. Yeh. Review of parameter identification procedures in groundwater hydrology: The inverse problem. *Water resources research*, 22(2):95–108, 1986.
- [32] C. yu Yang. Estimation of the temperature-dependent thermal conductivity in inverse heat conduction problems. *Applied Mathematical Modelling*, 23:469,478, 1999.